PERGAMON

MECHATRONICS

Mechatronics 11 (2001) 951–967

Adaptive robust controller design for multi-link flexible robots

T.H. Lee, S.S. Ge *, Z.P. Wang

Department of Electrical and Computer Engineering, National University of Singapore, 10 Kent Ridge Crescent, Singapore 117576, Singapore

Received 9 March 1999; accepted 31 May 2000

Abstract

Energy-based robust control strategy was proposed in [12] to improve the control performance of the traditional joint PD control by introducing additional control efforts through the evaluation of vibration related variables. Although the energy-based robust controller always guarantees closed-loop stability, it is not easy to find suitable gains of the terms for a satisfactory control performance. In this paper, adaptive energy-based robust control is presented for both closed-loop stability and automatic tuning of the gains of the additional control terms for desired performance. Simulation results are provided to show the effectiveness of the presented approach.

1. Introduction

For high speed positioning applications, light-weight manipulators are of considerable interest. With the promised advent of light-weight high strength composite materials, much attention has been given to modeling and control of flexible-link manipulators.

In order to improve industrial productivity, it is very desirable to build the robot link with light-weight material and thus increase the payload-to-weight ratio. When such a robot is carrying a large payload and moving at a high speed, the effect of link flexibility will be non-neglectable, and the traditional collocated control, e.g., the PD feedback is no longer sufficient for fast and accurate positioning. The system,

* Corresponding author. Tel.: +65-874-6821; fax: +65-779-1103.
E-mail address: elegesz@nus.edu.sg (S.S. Ge).

PII: S 0 9 5 7 - 4 1 5 8 (0 0) 0 0 0 6 2 - 3

described by partial differential equations (PDEs), is actually a distributed-parameter system of infinite dimensions. Its non-minimum phase behavior from the base input to the end-point output makes it very difficult to achieve high level performance and robustness simultaneously.

Various kinds of control techniques such as linear control [1], optimal control [2], adaptive nonlinear control [3], sliding mode control [4], feedback control [5], inverse dynamics method [6] and singular perturbation approach [7] have been investigated based on a truncated (finite dimensional) model obtained from either the Finite Element Method (FEM) or Assumed Modes Method (AMM). Some problems associated with the truncated-model-based methods have been highlighted in the literature such as controller/observer spillover problems [8]. To avoid such problems, some controllers are designed based on the partial differential equations directly, including direct strain feedback controller [8], quasi-tracking approach [9] and nonlinear vibration feedback controller [10].

Collocating the sensors and actuators at the joints of a flexible manipulator, for example the joint PD controller, can guarantee a certain degree of robustness of the closed-loop system. However, the performance of the flexible system with only a collocated controller is often not very satisfactory because the elastic modes of the flexible beam are seriously excited and not effectively suppressed. For this, non-collocated controller design have been obtained much interest.

Because the flexible link robot is governed by a set of partial differential equations, which means that the system is of infinite dimensionality, many control strategies that succeed in conventional rigid body robot control cannot be directly applied to solve the flexible robot control problem. In [12], an effective control strategy called energy-based robust control (EBRC) was proposed, which was constructed by introducing a robust term into the traditional collocated base PD controller. It was motivated by the fact that the link flexibility is not taken into consideration in the traditional PD control. Explicit evaluation of deflection related variables provides direct control efforts on vibration suppression. Although the energy-based robust controller always guarantees closed-loop stability, the performance may degrade significantly when the control gain of the robust term becomes small. Though any fixed large gain can guarantee good performance and fast stabilization, however, it is not recommended in practice. Large fixed gains would imply, in general, high noise amplification, high cost of control, and may be not necessarily needed. Therefore, one trade-off has to be made in performance improvement and feedback gain selection by trial and error.

Using adaptive techniques, the choice of the controller gain can be automatically tuned on-line. In [13], an adaptive direct strain feedback controller was proposed for a system driven by a direct drive DC motor of speed reference type only. In [14], an adaptive variable structure controller was constructed on the basis of a truncated model which, accordingly, may have the problems associated with truncated models including control and observation spillovers. Some self-tuning type adaptive control schemes were proposed in [15,16], where either ARMA or linear state space models were used for controller design by ignoring the nonlinear coupling effects. EBRC controller was derived from the basic energy-work relationship, thus, it is free from the drawbacks resulting from model uncertainties and model truncations. In order to improve the performance of EBRC controller, an adaptive energy-based robust controller is proposed by adaptively tuning the strain feedback gain rather than keeping the nonlinear feedback gain constant. Unlike the well known model-based adaptive control where it is required to estimate the physical parameters of the plant and then tune parameters of the controller adaptively, a simple adaptive gain tuning method is proposed for ease of implementation here.

The rest of the paper is organized as follows. The multi-link flexible robot is briefly introduced in Section 2. The adaptive energy-based robust controller design approach is presented in Section 3. Numerical simulation studies are carried out on a two-link flexible robot to verify the effectiveness of the controller in Section 4, followed by the conclusion in Section 5.

2. Multi-link flexible robot

We shall consider the flexible robots (i) deployed in space, or (ii) moving in the horizontal plane. In both cases, the effect of gravity is ignored for simplicity.

The N links are connected using N motors. Motor 1 is fixed in position, which is at the origin of the fixed base frame $X_1O_1Y_1$. The remaining motors, each being supported by a roller, are movable on the platform. The free tip of the last link has a payload attached.

For clarity, the geometry of the robot is shown in Fig. 1. There are totally $2N$ frames being used to describe the system, i.e., $X_iO_iY_i$ and $x_iO_iy_i$, $i = 1, 2, \ldots, N$. Frame $X_1O_1Y_1$, as stated above, is the fixed base frame. Other frames are all local reference frames attached to the corresponding motors, specifically axis O_iX_i

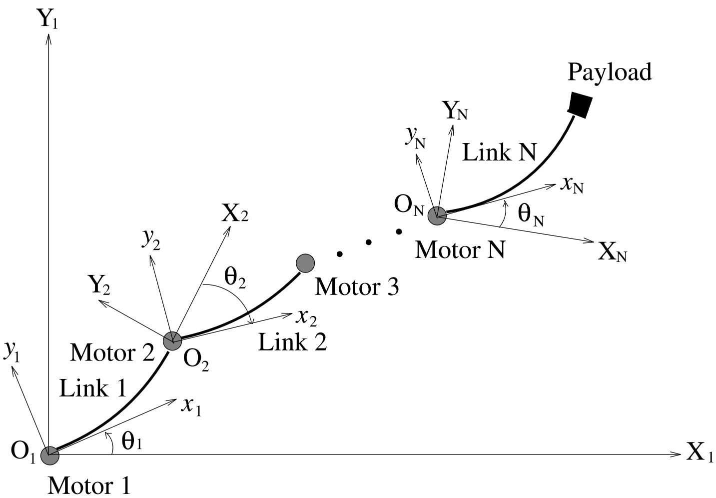

Fig. 1. Geometry of the multi-link flexible robot.

$(i = 2, 3, \ldots, N)$ is defined as the tangent to the end tip of link $i - 1$, and axis $O_i x_i$ $(i = 1, 2, \ldots, N)$ is tangent to link i at its base. The angular position of the ith link is denoted by θ_i measured in frame $X_i O_i Y_i$. θ_i is actually the angular difference between frames $x_i O_i y_i$ and $X_i O_i Y_i$.

For the system described above, the total work done by external inputs $W = \sum_{i=1}^{N} \int_0^t \tau_i(t)\dot{\theta}_i(t)\,\mathrm{d}t$. From the energy-work relationship, i.e., the increment of the system energy is equal to the work done by external inputs, we have the following equation [17]

$$[E_k(t) + E_p(t)] - [E_k(0) + E_p(0)] = \sum_{i=1}^{N} \int_0^t \dot{\theta}_i(t)\tau_i(t)\,\mathrm{d}t, \tag{2.1}$$

where $E_k(t)$ and $E_p(t)$ are the total kinetic energy and total potential energy of system at time t, $E_k(0)$ and $E_p(0)$ are constants representing the kinetic and potential energies at time 0. Therefore, by taking time derivatives of both sides of Eq. (2.1), we arrive at

$$\dot{E}_k(t) + \dot{E}_p(t) = \sum_{i=1}^{N} \dot{\theta}_i(t)\tau_i(t) \tag{2.2}$$

which will be used for the controller design in the following section.

3. Adaptive energy-based robust controller design

In this section, an adaptive energy-based robust controller is presented by further extending the results in [12]. The control objective here is to rotate each link of the robot to the desired angular position and simultaneously suppress the residual vibrations effectively.

Although the simple joint PD controller was shown to be able to stabilize the flexible robots [18], the system performance is not good because there is no explicit efforts introduced to suppress the residual vibrations. In [12], EBRC strategy for multi-link flexible robots was proposed by introducing one robust term where the vibration is evaluated explicitly and provides direct control effort on vibration suppression. As it has been shown that the gain of the nonlinear control term plays an important role in obtaining satisfactory performance. It was found that when the gain is too small, the control performance is very oscillatory. If the gain is too large, the control action may become not admissible. In addition, the existence of measurement noise also prohibit the use of high gain control. Unfortunately, it is very hard to find optimal gain of this robust term.

As we have mentioned at the beginning, our primary concern is to design a simple adaptive robust controller, while retaining the structure of energy-based robust controller for easy implementation. Therefore, instead of directly employing the conventional model-reference adaptive control, self-tuning adaptive control etc., we only propose to adaptively tune the control gain of the robust term in EBRC instead of keeping it constant as in [12].

First, let us consider the following strain feedback control law

$$\tau_i = -k_{pi}(\theta_i - \theta_{di}) - k_{di}\dot{\theta}_i - k_{si}y_i''(t,0)\mathrm{sgn}(\dot{\theta}_i)\int_0^t |\dot{\theta}_i|y_i''(s,0)\,\mathrm{d}s,$$
$$i = 1,2,\ldots,N, \tag{3.3}$$

where $y_i''(t,0)$ is the base strain of each link, $k_{si} = Y_{si}^2$ and Y_{si} is adaptively tuned by

$$\dot{Y}_{si}(t) = \alpha_i Y_{si}|\dot{\theta}_i|y_i''(t,0)\int_0^t |\dot{\theta}_i|y_i''(s,0)\,\mathrm{d}s - \sigma_i Y_{si}(t) \tag{3.4}$$

with k_{pi}, k_{di} and $\alpha_i > 0$, $i = 1,\ldots,N$. The σ-term in (3.4) is introduced to avoid divergence of the integral gains in the presence of disturbances. With the σ-term, $Y_{si}(t)$ is obtained as a first-order filtering of $\alpha_i Y_{si}|\dot{\theta}|y''(t,0)\int_0^t|\dot{\theta}|y''(s,0)\,\mathrm{d}s$.

Now, we are ready to present the following theorem on the stability of the multi-link flexible robot system.

Theorem 3.1. *Consider the multi-link flexible robot described in Section* 2. *Let the control objective be to rotate each link of the robot to the desired angular position*, *while simultaneously suppress the residual vibrations. Then*, *the proposed control law* (3.3) *and the adaptation law* (3.4) *can guarantee the stability of the closed-loop multi-link flexible robotic system.*

Proof. Consider the following Lyapunov function candidate

$$V = E_k + E_p + \frac{1}{2}\sum_{i=1}^{N}k_{pi}(\theta_i - \theta_{di})^2 + \frac{1}{2}\sum_{i=1}^{N}\alpha_i^{-1}Y_{si}^2. \tag{3.5}$$

By virtue of Eq. (2.2), the time derivative of V is given by

$$\dot{V} = \sum_{i=1}^{N}\tau_i\dot{\theta}_i + \sum_{i=1}^{N}k_{pi}(\theta_i - \theta_{di})\dot{\theta}_i + \sum_{i=1}^{N}\alpha_i^{-1}Y_{si}\dot{Y}_{si}.$$

Substituting the control law (3.3) and the adaptation law (3.4) into the above equation, we have

$$\begin{aligned}\dot{V} = &\sum_{i=1}^{N}\left\{-k_{pi}(\theta_i - \theta_{di}) - k_{di}\dot{\theta}_i - k_{si}y_i''(t,0)\mathrm{sgn}(\dot{\theta}_i)\int_0^t|\dot{\theta}_i|y_i''(s,0)\,\mathrm{d}s\right\}\dot{\theta}_i \\ &+ \sum_{i=1}^{N}k_{pi}(\theta_i - \theta_{di})\dot{\theta}_i + \sum_{i=1}^{N}\alpha_i^{-1}Y_{si}\left\{\alpha_i Y_{si}|\dot{\theta}|y_i''(t,0)\int_0^t|\dot{\theta}|y_i''(s,0)\,\mathrm{d}s - \sigma_i Y_{si}(t)\right\} \\ = &-\sum_{i=1}^{N}k_{di}\dot{\theta}_i^2 - \sum_{i=1}^{N}\alpha_i^{-1}\sigma_i Y_{si}^2 \leqslant 0.\end{aligned} \tag{3.6}$$

It follows that $0 \leqslant V(t) \leqslant V(0)\ \forall t \geqslant 0$, hence $V(t) \in L_\infty$. Since $V(t)$ is a continuous function of Y_{si}, $V(t)$ is non-increasing in t, which implies the boundedness of Y_{si} and, hence, the boundedness of k_{si}. In addition, it also implies that the closed-loop system is energy dissipative and, hence, stable. □

Remarks.

1. The joint PD controller for the ith link is a special case of the τ_i in (3.3) by setting k_{si}'s to be fixed at zeros. The introduction of the k_{si} items allows us to explicitly consider the bending of the flexible beam, and subsequently have direct control effect on elastic vibrations.
2. From (3.3), one can easily see that only the measurements of the joint angle θ_i, joint velocity $\dot{\theta}_i$, and base strain signal of each link are needed. The joint position θ_i and the joint velocity $\dot{\theta}_i$ can be obtained by rotary encoder and tachometer attached to the rotor of motor i, base strain signal can be obtained through the strain gauge [12]. Therefore, the controller is very easy to implement from the engineering point of view.
3. The stability proof is independent of the system dynamics and thus the drawbacks/problems, such as control and observation spillovers, associated with model-based controllers mentioned in Section 1 are avoided.
4. Because the bending strain signals $y_i''(0,t)$ are chosen in the local reference frame $x_iO_iy_i$, such as those aforementioned, the controller presented in (3.3) are of decentralized type, which has the advantages of requiring few computer resources, and giving ease of implementation and tolerance to failure, since the N controllers in (3.3) can be implemented in parallel [12].
5. In control law (3.3) and adaptation law (3.4), only base strain was used to construct the nonlinear term. However, it can be easily extended to the general control where a general function $f_i(x,t)$ is used instead of $y_i''(0,t)$. Some examples of function $f_i(x,t)$ of link i described in frame $x_iO_iy_i$ are $y_i(x_i,t)$ (deflection at x_i), $y_i'(x_i,t)$ (rotation at x_i), $y_i''(x_i,t)$ (strain at x_i), and $y_i'''(x_i,t)$ (shearing force at x_i) $\forall x_i \in [0, L_i]$ where L_i is the length of the ith link [12].
6. As a matter of fact, the controller can be further generalized to cases of multiple feedbacks as follows:

$$\tau_i = -k_{pi}(\theta_i - \theta_{di}) - k_{di}\dot{\theta}_i - \sum_{j=1}^{m_i} k_{sij} f_i(t, x_{sij})\ \mathrm{sgn}(\dot{\theta}_i) \int_0^t |\dot{\theta}_i| f_i(s, x_{sij})\,\mathrm{d}s,$$
$$i = 1, 2, \ldots, N, \tag{3.7}$$

where $k_{sij} = Y_{sij}^2$ and Y_{sij} is adaptively tuned by

$$\dot{Y}_{sij}(t) = \alpha_{ij} Y_{sij} |\dot{\theta}_i| f_i(t, x_{sij}) \int_0^t |\dot{\theta}_i| f_i(s, x_{sij})\,\mathrm{d}s - \sigma_{ij} Y_{sij}(t) \tag{3.8}$$

with $j = 1, 2, \ldots, m_i$, and $x_{sij} \in [0, L_i]$ being the location of the jth sensor on the ith link. The stability of the closed-loop system can be shown easily by choosing the following Lyapunov function candidate

$$V = E_k + E_p + \frac{1}{2}\sum_{i=1}^{N} k_{pi}(\theta_i - \theta_{di})^2 + \frac{1}{2}\sum_{i=1}^{N}\sum_{j=1}^{m_i} \alpha_{ij}^{-1} Y_{sij}^2. \tag{3.9}$$

7. It should be noted that the bending variables associated with other links can also be introduced into the feedback of link i without destabilizing the system. For example, assuming that only base strain of each link can be obtained, then the controller can be given by

$$\tau_i = -k_{pi}(\theta_i - \theta_{di}) - k_{di}\dot{\theta}_i - \sum_{j=1}^{N} k_{sij} y_j''(t,0)\ \mathrm{sgn}(\dot{\theta}_i) \int_0^t |\dot{\theta}_i| y_j''(s,0)\ \mathrm{d}s,$$

$$i = 1, 2, \ldots, N, \tag{3.10}$$

where $k_{sij} = Y_{sij}^2$ and Y_{sij} is adaptively tuned by

$$\dot{Y}_{sij}(t) = \alpha_{ij} Y_{sij} |\dot{\theta}_i| y_j''(t,0) \int_0^t |\dot{\theta}_i| y_j''(s,0)\ \mathrm{d}s - \sigma_{ij} Y_{sij}(t).$$

The stability of the closed-loop system can be shown by choosing the following Lyapunov function candidate

$$V = E_k + E_p + \frac{1}{2}\sum_{i=1}^{N} k_{pi}(\theta_i - \theta_{di})^2 + \frac{1}{2}\sum_{i=1}^{N}\sum_{j=1}^{N} \alpha_{ij}^{-1} Y_{sij}^2.$$

Note that controllers (3.7) and (3.10) are centralized rather than decentralized. Based on the same idea, controllers of similar forms can be easily formed and investigated.

Although the stability of the closed-loop system has been given, it is difficult to achieve asymptotic stability. This is mainly due to the infinite dimensionality of the system. If the system is of finite dimensions, then LaSalle's theorem can be used to prove the asymptotic stability.

Theorem 3.2. *The proposed control law* (3.3) *and the adaptation law* (3.4) *can guarantee the asymptotic stability of the closed-loop truncated system*, *which is obtained through representing the deflection of each link by an arbitrary finite number of flexible modes*.

Proof. See Appendix A. □

Remarks.

1. Although model-truncation has also been invoked in proving the asymptotic stability in Theorem 3.2, controller (3.3) with adaptive law (3.4) has some significant differences from the traditional truncated-model-based ones: (a) since controller (3.3) is not of states-feedback type, reconstruction of flexible modes is not necessary and thus the problem of control/observation spillovers, which is caused by ignoring high frequency modes in controller and observer design, does not exist; (b) asymptotic stability can be guaranteed for a truncated system with an *arbitrary* finite number of flexible modes (Theorem 3.2) without the need to increase the order of the controller, and thus the computing burden can be always kept light; and (c) the controller allows great freedom in feedback design and is very easy to implement, since the vibration feedback signals can be chosen according to available sensor facilities, and no high order signal measurements are needed.
2. Though the asymptotical stability is proved for controller (3.3) with adaptive law (3.4), the same conclusions can be drawn for other general controllers (3.7) and (3.10).

4. Simulation studies

In this section, some numerical simulations are carried out on a two-link flexible robot. The plant is simulated by a FEM model in which each link is divided into four elements with the same length. A fourth-order Runge–Kutta program with adaptive step-size is used to numerically solve the differential equations. The sampling interval is set to be 0.01 s. To take into account of the limited bandwidth of the actuators, control signal is filtered by a low pass filter, i.e., only those low frequency components below 100 Hz in the control signals will be applied to the system.

The system parameters are given in Table 1, in which M_{t1} actually denotes the 2nd motor, and M_{t2} is the payload attached to the end tip of link 2.

The initial joint positions of the both links are all zeros, and the set point values of the two links are $\theta_{d1} = 20°$ and $\theta_{d2} = 10°$. The robot is assumed to be initially at rest without any deformation.

Following the discussion in [12], let the traditional PD control be

$$\tau_{\mathrm{PD}i} = -k_{pi}(\theta_i - \theta_{di}) - k_{vi}\dot{\theta}_i, \quad i = 1, 2.$$

It is already known that for any $k_{pi}, k_{di} > 0$ will not destabilize the closed-loop system. However, different selection of k_{pi} and k_{vi} will lead to very different performance. By taking smart materials links as rigid, k_{pi} and k_{di} are selected to make the closed-loop critically damped. The corresponding rigid motion error equation of the smart materials links is

$$I_{\mathrm{e}i}\ddot{e}_i(t) + k_{di}\dot{e}_i(t) + k_{pi}e_i = 0, \quad i = 1, 2,$$

where $I_{\mathrm{e}i}$ represents the equivalent inertia of the ith joint, $e_i = \theta_i - \theta_{di}$, and $\ddot{e}_i = \ddot{\theta}_i$ and $\dot{e}_i = \dot{\theta}_i$ since θ_{di} is constant. It should be noted that because of the rotational movement of the 2nd link, $I_{\mathrm{e}1}$ is not constant even when the two links are all assumed to be rigid. For simplicity, in our simulations, $I_{\mathrm{e}1}$ is determined by further assuming that motor 2 is locked at $\theta_2 = 0$, i.e., the two links are align. Subsequently, we have $I_{\mathrm{e}1} = 3.46$ kg m^2 and $I_{\mathrm{e}2} = 1.55$ kg m^2. For the second-order systems above, if critical damping is assumed ($\xi = 1$), then $k_{pi} = I_{\mathrm{e}i}\omega_{ni}^2$ and $k_{vi} = 2I_{\mathrm{e}i}\omega_{ni}$, ω_{ni} $(i = 1, 2)$ are the corresponding natural frequencies. Choosing $\omega_{n1} = 2.5$ and $\omega_{n2} = 3.0$, we have

$$\tau_{\mathrm{PD}1} = -21.6(\theta_1 - \theta_{d1}) - 17.3\dot{\theta}_1, \tag{4.11}$$

$$\tau_{\mathrm{PD}2} = -14.0(\theta_2 - \theta_{d2}) - 9.3\dot{\theta}_2. \tag{4.12}$$

Table 1
System parameters

	Link 1	Link 2
Length	$L_1 = 1.0$ m	$L_2 = 0.8$ m
Flexural rigidity	$EI_1 = 5.0$ Nm^2	$EI_2 = 3.0$ Nm^2
Linear density	$\rho_1 = 0.1$ kg m^{-1}	$\rho_2 = 0.1$ kg m^{-1}
Hub initial	$I_{h1} = 3.0$ kg m^2	$I_{h2} = 1.5$ kg m^2
Payload	$M_{t1} = 0.1$ kg	$M_{t2} = 0.05$ kg

The EBRC in [12] is given by

$$\tau_i = \tau_{\mathrm{PD}i} - k_{si} y_i''(0,t) \int_0^t |\dot{\theta}_i(s)| y_i''(0,s)\, \mathrm{d}s, \quad i = 1, 2, \tag{4.13}$$

where $y_i''(0,t)$ are the base strain feedback for each link.

While the adaptive energy-based robust controller (AERC) used for simulation study is given by

$$\tau_i = \tau_{\mathrm{PD}i} - k_{si} y_i''(0,t) \int_0^t |\dot{\theta}_i(s)| y_i''(0,s)\, \mathrm{d}s \tag{4.14}$$

with $k_{si} = Y_{si}^2$ and the adaptation law of Y_{si} is

$$\dot{Y}_{si}(t) = \alpha_i Y_{si} |\dot{\theta}_i| y_i''(t,0) \int_0^t |\dot{\theta}_i| y_i''(s,0)\, \mathrm{d}s - \sigma_i Y_{si}(t), \quad i = 1, 2. \tag{4.15}$$

Fig. 2 shows the tip deflections of EBRC with different fixed gains, say $k_{si} = 100$, 1000 and 5000, and the AERC with $\alpha_1 = 4 \times 10^4$ and $\alpha_2 = 6 \times 10^4$, $\sigma_i = 0.1$ and $k_{si}(0) = 1000$. It can be seen that EBRC controller with $k_{si} = 100$ gives the worst performance while the EBRC with higher k_{si} can suppress the residual vibration effectively. However, high gain is not desirable from a practical point of view. It can

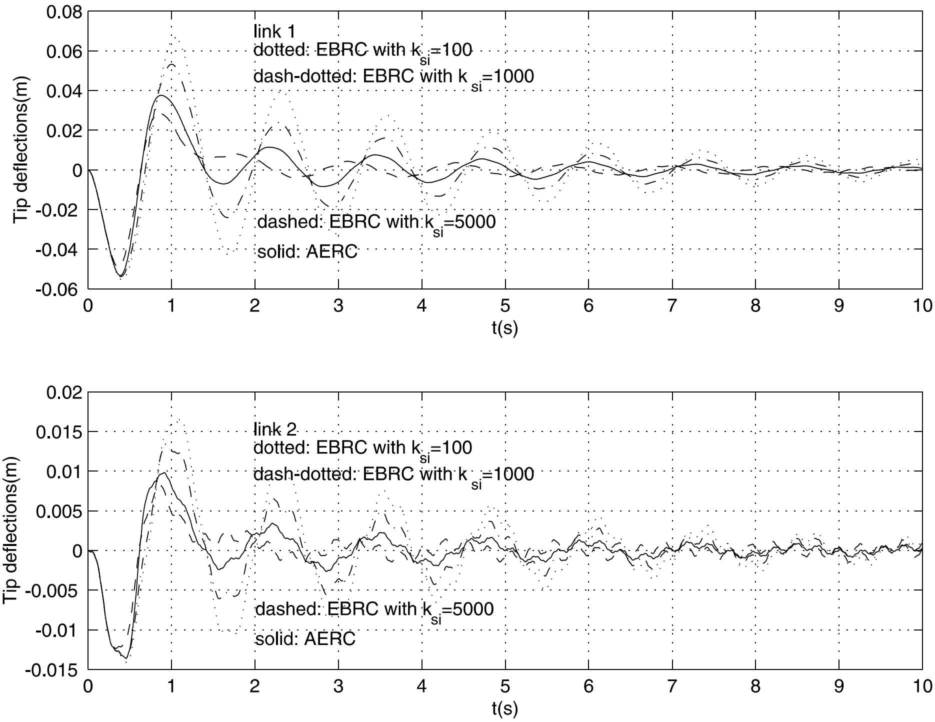

Fig. 2. Tip deflections under EBRCs and AERC.

be seen that the AERC can also achieve comparatively good performance while k_{si} is adjusted adaptively.

Fig. 3 shows changes of k_{si} in gain adaptive robust controller. The maximum values of k_{s1} and k_{s2} are 6699 and 1418, respectively, and the minimum values of k_{s1} and k_{s2} are 370 and 388, respectively. It can be seen that k_{si} are relatively high at the beginning, then with the residual vibrations become small, k_{si} also become small. k_{si} will converge to zero as time approaches infinity. This is very desirable in engineering practice.

What we care about most in tip position control is the tip trajectories, which are required to converge fast with as small vibrations/overshoots as possible to improve positioning accuracy. Under the assumption of small deflection, the tip position of the two links can be approximated by

$$p_1 = L_1\theta_1 + y_1(L_1, t),$$
$$p_2 = L_2\theta_2 + y_2(L_2, t)$$

in which the angular displacements θ_1 and θ_2 should be represented in radians instead of degrees. The tip positions p_1 and p_2 are plotted in Fig. 4. It is seen that the tip trajectories of gain adaptive robust control are quite good since it is smooth, converging fast and there are very little vibrations and overshoots.

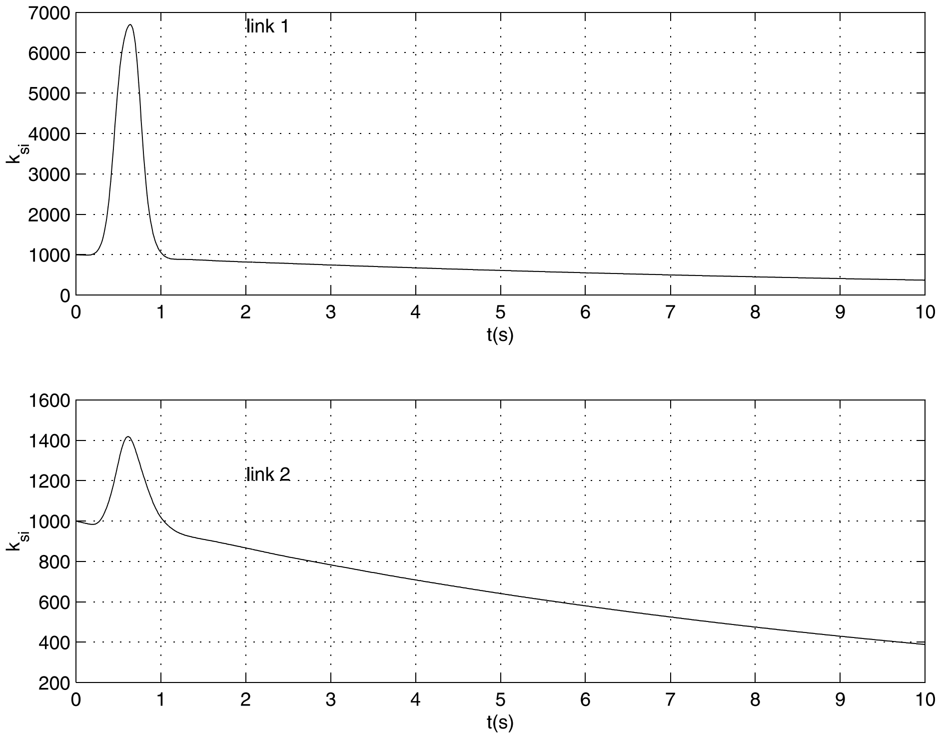

Fig. 3. Changes of k_{si} in AERC.

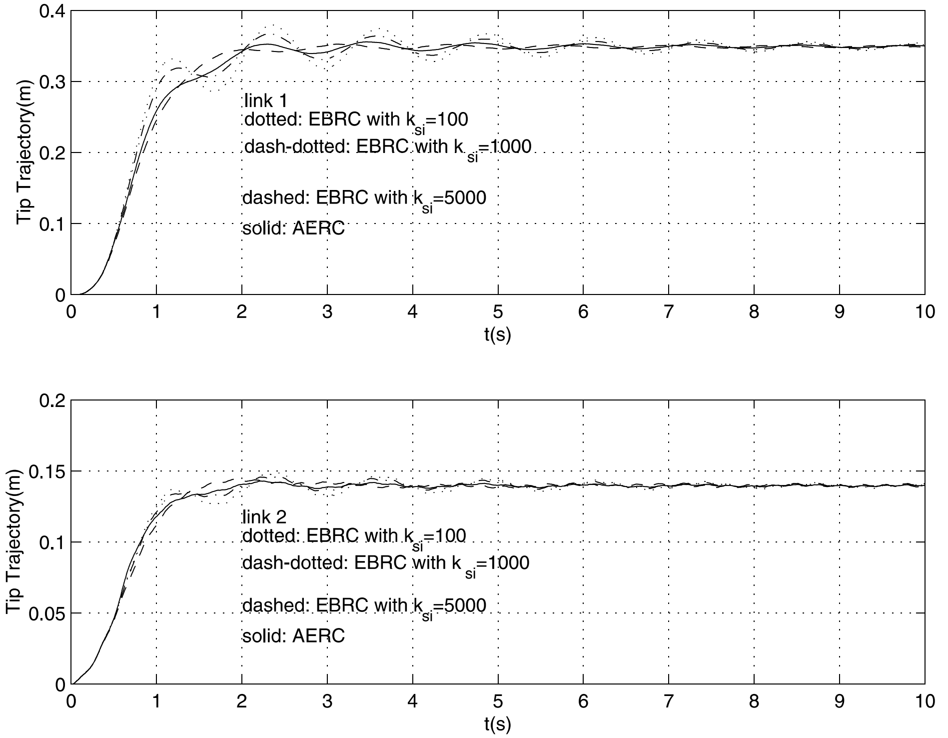

Fig. 4. Tip trajectory under EBRCs and AERC.

For better understanding, and a clear presentation, other signals in the closed-loop are compared between the EBRC with different k_{si}s and the gain adaptive robust controller. Fig. 5 shows the joint angle response, while Fig. 6 shows the control torque. It can be seen that all signals in the closed-loop are bounded.

In the above, through simulations, we have shown the effectiveness of the controller in (4.14) and (4.15). It should be pointed out that other kinds of signals or other kinds of combinations of signals can also be considered depending on the available sensor facilities, since the controller in (4.14) and (4.15) actually allows great freedom of feedback design.

5. Conclusion

In this paper, gain adaptive robust regulation for multi-link flexible robots has been presented. Theoretical proofs have shown that closed-loop system is stable, and the controller is independent of system parameters and hence possess stability robustness to parameter variations. Furthermore the controller can be easily

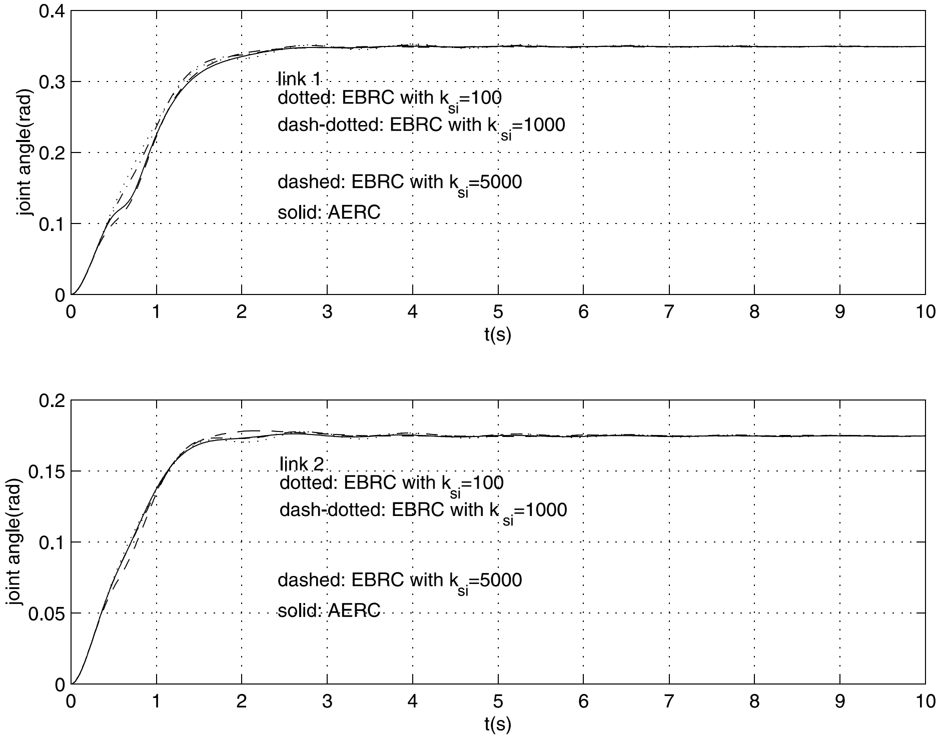

Fig. 5. Joint angle under EBRCs and AERC.

implemented because the signals used in the feedback control can be measured directly or be chosen as measurable ones. Numerical simulations have shown that system response converges fast and the residue vibrations are effectively suppressed using the controller proposed.

Appendix A. Proof of Theorem 3.2

It can be easily proven by following the procedures in [11]. It is given here for completeness and easy reference. Using the same Lyapunov functions (3.5), we consider the motion of the system in the largest invariant set in the set $\dot{V} = 0$. Then we have $\dot{\theta}_i \equiv 0$ and $Y_{si} \equiv 0$, hence, $k_{si} \equiv 0$. Subsequently, $\ddot{\theta}_i = 0$, $\tau_i = -k_{pi}(\theta_i - \theta_{di})$, $i = 1, 2, \ldots, N$.

Firstly, consider link 1. With the aid of the notable Hamilton's principle, considering the motion of system in $\dot{V} = 0$, we have the following PDEs of link 1

$$EI_1 y_1''(0,t) - k_{p1}(\theta_1 - \theta_{d1}) = 0, \tag{A.1}$$

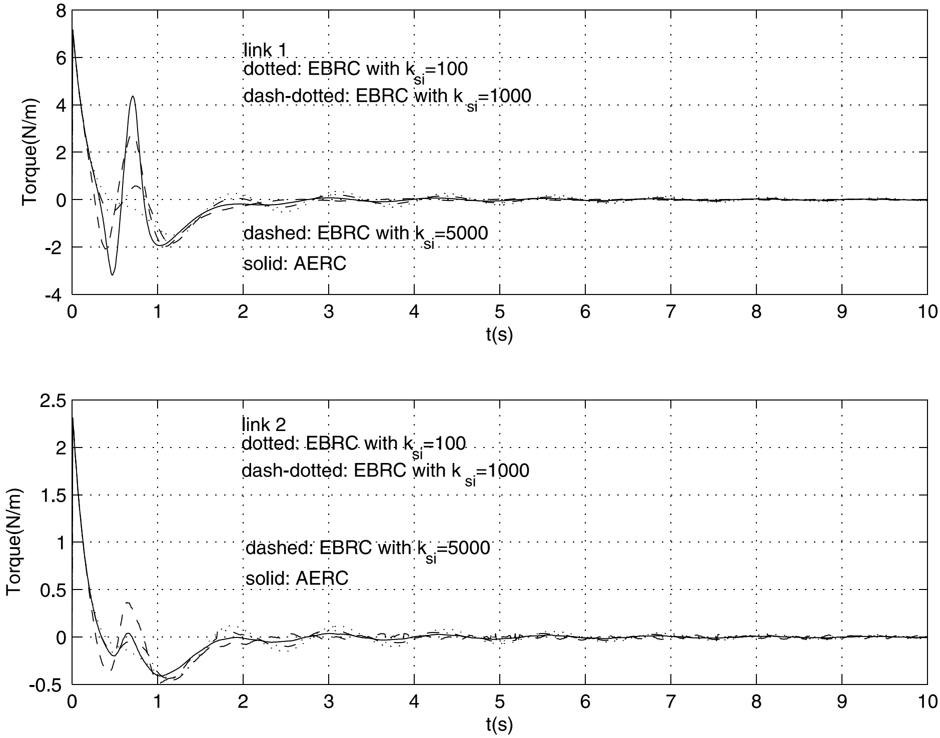

Fig. 6. Control torque under EBRCs and AERC.

$$\rho_1 \ddot{y}_1(x_1, t) = -EI_1 y_1''''(x_1, t), \quad 0 \leqslant x_1 \leqslant L_1 \tag{A.2}$$

and boundary conditions (BCs) of link 1

$$y_1(0, t) = 0, \quad y_1'(0, t) = 0, \tag{A.3}$$

$$y_1''(0, t) = \frac{k_{p1}}{EI_1}(\theta_1 - \theta_{d1}). \tag{A.4}$$

Because $\dot{\theta}_i \equiv 0$, the robot is operated as if all the motors are locked. Consequently, each motor can be taken simply as a concentrated mass. Hence, the bending moment at the tip of link $i-1$ should be equal to the base bending moment of link i, i.e.,

$$EI_{i-1} y_{i-1}''(L_{i-1}, t) = EI_i y_i''(0, t), \quad i = 2, 3, \ldots, N.$$

Considering links 1 and 2, and noting that

$$EI_2 y_2''(0, t) = -\tau_2 = k_{p2}(\theta_2 - \theta_{d2})$$

then, we have another boundary condition

$$y_1''(L_1, t) = \frac{k_{p2}}{EI_1}(\theta_2 - \theta_{d2}). \tag{A.5}$$

It is noted that the left-hand sides of Eqs. (A.4) and (A.5) are functions of time, while the right-hand sides are constants. Let us firstly assumed that the two constants are zero. It is shown later that either constants being non-zero leads to invalid solutions. Now Eqs. (A.4) and (A.5) can be rewritten as

$$y_1''(0,t) = 0, \tag{A.6}$$

$$y_1''(L_1,t) = 0. \tag{A.7}$$

Using the Method of Separating Variables [19], the solution to (A.2) is assumed to be of the form $y(x,t) = \Psi(x)Q(t)$, and Eq. (A.2) becomes

$$\frac{\Psi''''(x)}{\Psi(x)} \cdot \frac{EI_1}{\rho_1} = -\frac{\ddot{Q}(t)}{Q(t)}, \tag{A.8}$$

where primes denote the derivatives of x and dots denote the derivatives of t. It is clear that the left-hand side of Eq. (A.8) is a pure function of x while the right-hand side depends on t only. Therefore, both sides of Eq. (A.8) should be equal to a constant. If k is used to denote the constant, the PDE (A.8) can be reduced into two ordinary differential equations (ODEs), namely

$$\ddot{Q}(t) = -kQ(t), \tag{A.9}$$

$$\Psi''''(x_1) = \frac{\rho_1}{EI_1} k \Psi(x_1). \tag{A.10}$$

The BCs become

$$\begin{aligned} &\Psi(0) = 0, \\ &\Psi'(0) = 0, \\ &\Psi''(0) = 0, \\ &\Psi''(L_1) = 0. \end{aligned} \tag{A.11}$$

We will consider Eq. (A.10) and conditions (A.11) with regard to different values of the constant k.

It can be proved that when $k = 0$ and $k > 0$, the solution to Eq. (A.10) is trivial. Then we just need to consider the case for $k < 0$.

Letting $k = -\omega^2 < 0$, Eq. (A.10) can be rewritten as

$$\Psi''''(x_1) = -\left(\frac{v}{L}\right)^4 \Psi(x_1) \tag{A.12}$$

with

$$\left(\frac{v}{L}\right)^4 = \omega^2 \frac{\rho_1}{EI_1}. \tag{A.13}$$

The general solution to Eq. (A.12) is of the form

$$\Psi(x_1) = C_1 e^{ax_1} \sin(ax_1) + C_2 e^{ax_1} \cos(ax_1) + C_3 e^{-ax_1} \sin(ax_1) + C_4 e^{-ax_1} \cos(ax_1), \tag{A.14}$$

where $a = v/\sqrt{2}L_1$. From BCs (A.11), a set of equations are obtained

$$\begin{aligned} &C_2 + C_4 = 0, \\ &C_1 + C_2 + C_3 - C_4 = 0, \\ &C_1 - C_3 = 0, \\ &(C_1 e^{aL_1} - C_3 e^{-aL_1})\cos(aL_1) - (C_2 e^{aL_1} - C_4 e^{-aL_1})\sin(aL_1) = 0. \end{aligned} \tag{A.15}$$

To obtain non-trivial solutions, the determinant of the coefficient matrix of Eqs. (A.15) must be zero, i.e.,

$$4(\sin(aL_1)\cosh(aL_1) + \cos(aL_1)\sinh(aL_1)) = 0 \tag{A.16}$$

which may be satisfied by an infinite number of a. Consider only positive a_i, an infinite number of solutions to the boundary value problem can be given by

$$\begin{aligned} \Psi_i(x_1) = {} & C_1^i e^{a_i x_1}\sin(a_i x_1) + C_2^i e^{a_i x_1}\cos(a_i x_1) + C_3^i e^{-a_i x_1}\sin(a_i x_1) \\ & + C_4^i e^{-a_i x_1}\cos(a_i x_1), \end{aligned}$$

where $C_1^i \sim C_4^i$ denote the solution to Eq. (A.15) corresponding to a_i.

When $k = -\omega^2$ with ω being non-zero number, the solution to Eq. (A.9) can be obtained

$$q_i(t) = D_1^i e^{\omega_i t} + D_2^i e^{-\omega_i t}, \tag{A.17}$$

where D_1^i and D_2^i are related to the initial conditions of $y_1(x_1, t)$. Note that the "initial" moment t_0 should denote the moment when the system motion enters the invariant set, rather than the initial operating moment since we are considering the motion of the system in the largest invariant set in the set $\dot{V} = 0$. Then from the Superposition or Linearity Principle [19], a solution $y(x, t)$ can be given by

$$y(x_1, t) = \sum_{i=1}^{\infty} \psi_i(x_1) q_i(t). \tag{A.18}$$

Note that the ω_i in Eq. (A.17) can be either positive or negative, without loss of generality, if $\omega_i \geqslant 0$. This leads to $D_1^i = 0$ as follows. If $D_1^i \neq 0$, then $\lim_{t\to\infty} q_i(t) \to \infty$ and $\lim_{t\to\infty} \dot{q}_i(t) \to \infty$, and hence $\lim_{t\to\infty} \dot{y}_1(x_1, t) \to \infty$. This implies the kinetic energy E_k of the system approaches infinity, which contradicts the fact the V in Eq. (3.5) is actually bounded. Therefore, D_1^i must be zero. Consequently, when $k < 0$, the solution (A.18) approaches zero as time approaches infinity.

In summary, $y_1(x_1, t) = 0$ provided that the system motion is in the largest invariant set $\dot{V} = 0$. Moreover, recalling that we already have $\theta_1 = \theta_{d1}$, we further conclude that if the system motion is in the largest invariant set $\dot{V} = 0$, the first link must stop in the final position described by $\theta_1 = \theta_{d1}$ and $y_1(x_1, t) = 0$. Then in this case, the local frame $X_2O_2Y_2$ is actually static with respect to the inertia frame $X_1O_1Y_1$. This allows us to take $X_2O_2Y_2$ as the inertia frame in which the second link is to be considered. Then we have the following PDEs of link 2

$$EI_2 y_2''(0, t) - k_{p2}(\theta_2 - \theta_{d2}) = 0, \tag{A.19}$$

$$\rho_2 \ddot{y}_2(x_2, t) = -EI_2 y_2''''(x_2, t), \quad 0 \leqslant x_2 \leqslant L_2. \tag{A.20}$$

Moreover, from Fig. 1 and the above conclusions, a set of boundary conditions similar to (A.3), (A.6) and (A.7) also exist for Eq. (A.20), i.e.,

$$y_2(0,t) = 0, \quad y_2'(0,t) = 0, \quad y_2''(0,t) = 0, \quad y_2''(L_2,t) = 0.$$

Thus carrying out similar analysis for link 2 leads to the conclusion that link 2 must stop at its final position described by $\theta_2 = \theta_{d2}$ and $y_2(x_2,t) = 0$ provided that the system motion is in the largest invariant set $\dot{V} = 0$. This implies the local frame $X_3O_3Y_3$ can be considered as the inertia frame for link 3. Now it is easy to see that repeating the same procedure until link N finally leads to the fact that if the system motion is in the largest invariant set $\dot{V} = 0$, then all links must stop at their final positions, i.e., $\theta_i = \theta_{di}$ and $y_i(x_i,t) = 0$ $(i = 1,2,\ldots,N)$.

Now, let us consider the case when the right-hand side of either Eq. (A.4) or (A.5) is a non-zero constant is discussed. If this is true, then from $y_1(x_1,t) = \Psi(x_1)Q(t)$, $Q(t)$ and hence $y_1(x_1,t)$ must be constant. This means that the first link is static, which implies that the right-hand side of both Eqs. (A.4) and (A.5) must equal the same non-zero constant (from the moment balance of a static bending beam). Subsequently, frame $X_2O_2Y_2$ can be taken as the inertia frame for link 2. Because the base bending moment of link 2 equals the tip bending moment of link 1 (note the condition $\dot{V} = 0$), the base bending moment of link 2 must be the same constant. This, by assuming $y_2(x_2,t) = \Psi(x_2)Q(t)$, implies link 2 is also static. Repeating the same procedures for all links leads to a static bending N-link robot. Then from the moment balance of the static robot, the base bending moment of link 1 should be equal to the tip bending moment of link N. Since the free tip of link N is loaded with a concentrated mass, the tip bending moment is zero. Therefore either the base bending moment of link 1 or its tip bending moment must be zero.

Now invoking the truncation assumption, the elastic deflection of each link is assumed to be described by a finite number of flexible modes, and subsequently the system is of only finite dimensions. For this truncated system, because it has been proven already that the largest invariant set $\dot{V} = 0$ is the final equilibrium position, the asymptotic stability directly follows the LaSalle's theorem. □

References

[1] Cannon Jr RH, Schmitz E. Initial experiments on the end-point control of a flexible robot. Int J Robotics Res 1984;3(3):62–75.

[2] Arakawa A, Fukuda T, Hara F. H_∞ control of a flexible robotics arm (effect of parameter uncertainties on stability). IEEE/RSJ International Workshop on Intelligent Robots and Systems IROS '91. p. 959–64.

[3] Yang JH, Lian FL, Fu LC. Nonlinear adaptive control for flexible-link manipulators. IEEE Trans Robotics Automation 1997;13(1):140–6.

[4] Chen YP, Yeung KS. Regulation of a one-link flexible robot arm using sliding-mode technique. Int J Control 1989;49:1965–78.

[5] Sakawa Y, Matsuno F, Fukushima S. Modelling and feedback control of a flexible arm. J Robotic Syst 1985;2(4):453–72.

[6] Morris AS, Madani A. Computed torque control applied to a simulated two-flexible-link robot. Trans Inst MC 1997;19(1):50–60.

[7] Siciliano B, Book WJ. A singular perturbation approach to control of lightweight flexible manipulator. Int J Robotics Res 1988;7(4):79–89.
[8] Luo ZH. Direct strain feedback control of flexible robot arm: new theoretical and experimental results. IEEE Trans Automatic Control 1993;38(11):1610–22.
[9] Zhu G, Ge SS. A quasi-tracking approach for finite-time control of a mass-beam system. Automatica 1998;34(7):881–8.
[10] Ge SS, Lee TH, Zhu G. Asymptotically stable end-point regulation of a flexible SCARA/Cartesian robot. IEEE/ASME Trans Mechatronics 1998;3(2):138–44.
[11] Ge SS, Lee TH, Zhu G. Non-model-based position control of a planar multi-link flexible robot. Mechanical Syst Signal Process 1997;11(5):707–24.
[12] Ge SS, Lee TH, Zhu G. Energy-based robust controller design for multi-link flexible robots. Mechatronics 1996;6(7):779–98.
[13] Luo ZH, Sakawa Y. Gain adaptive direct strain feedback control of flexible robot arms. In: Proceedings of IEEE Region 10 Conference, TENCON '93. China: Beijing; 1993. p. 199–202.
[14] Yang JH, Lian FL, Fu LC. Adaptive robust control of flexible manipulators. In: Proceedings of IEEE International Conference on Robotics and Automation; 1995. p. 1223–28.
[15] Nemier D, Koivo AJ, Kashyap RJ. Control of gripper position of a compliant link using strain gauge measurements. In: Proceedings of IEEE Conference on Decision and Control; 1986. p. 1140–44.
[16] Chen JS, Meng CH. Modeling and adaptive control of a flexible one-link manipulator. Robotica 1990;8:339–45.
[17] Hammond P. Energy methods in electromagnetism. Oxford: Clarendon Press; 1981.
[18] Yigit AS. On the stability of PD control for a two-link rigid-flexible manipulator. ASME J Dynam Syst, Meas Control 1994;116:179–85.
[19] Meirovitch L. Elements of vibration analysis. 2nd ed. New York: McGraw-Hill; 1986 [chapters 7 and 8].